Korean J. Chem. Eng., 40(12), 3039-3045 (2023)
DOI: 10.1007/s11814-023-1515-y

pISSN: 0256-1115
eISSN: 1975-7220

Infrared initiation of frontal polymerization with density variation multi-layered resins for variable colored layers via photothermal effect

Ensoo Wi and Younghun Kim†

Department of Chemical Engineering, Kwangwoon University, 20 Kwangwoon-ro, Nowon-gu, Seoul 01897, Korea
(*Received 26 March 2023 • Revised 7 June 2023 • Accepted 19 June 2023*)

Abstract−Frontal polymerization (FP) is a unique polymerization technique that involves the self-propagation of heat, which is triggered by a local heat source, such as a photoinitiator. We propose here a novel method for producing colorful polymeric layers through an FP reaction using carbon black (CB) under near-infrared (NIR) irradiation. In the FP reaction, CB and dicyclopentadiene (DCPD) were used as the photothermal agent and monomer, respectively. The photothermal efficiencies of the CB/DCPD suspensions were found to increase with the increase in their CB content. After photothermal initiation, the exothermic FP reaction propagated thermally, resulting in the formation of a free-standing poly (DCPD) resin. In addition, the density of the DCPD suspension in the test tube was adjusted to prepare a multilayered, colored poly (DCPD) resin. Consequently, a four-colored poly (DCPD) resin was obtained via an NIR-induced FP reaction. These results indicate that nanosized CB can be an effective photothermal agent for FP and that the proposed approach can be used for the rapid curing of polymers with multicolored layers with low energy consumption.

Keywords: Photothermal, Infrared, Frontal Polymerization, Dicyclopentadiene, Carbon Black

INTRODUCTION

Frontal polymerization (FP) involves the propagation of a self-sustaining reaction wave, which is powered by heat and chemical reaction [1-5]. This method offers several advantages over traditional polymerization methods, including faster reaction rates, lower energy consumption, and easier process control. Consequently, FP has attracted considerable interest as a promising method for producing high-performance polymer composites, coatings, and adhesives [2].

FP occurs spontaneously when a high-energy initiator is positioned at the leading edge of a monomer [3]. As soon as the reaction begins, sufficient heat is produced to maintain the polymerization front and to spread it throughout the monomer or prepolymer material. This exothermic reaction can be sustained and spread without requiring any additional external energy input because the energy source for FP comes from this reaction [4]. Unlike conventional polymerization techniques, this method enables the quick formation of intricate shapes and structures without the use of molds or other shaping tools and is capable of polymerizing a variety of monomer mixtures, including those that are challenging or impossible to perform using conventional techniques [5].

The exothermic reaction is usually triggered by a local heat source, such as an external heating element [6]. However, FP can also be initiated by using other energy sources. A new FP method called frontal photopolymerization has been developed, which uses a chemical substance that reacts with light, such as a photoinitiator, to initiate a reaction [7]. Photoinitiator molecules absorb energy from light and are transformed into reactive intermediates. When these intermediates propagate, photopolymerization occurs, and heat is generated during the process.

In general, light-induced FP is more favorable than heat-induced FP because it enables noncontact and remote initiation and can lead to facile multipoint initiation [1]. Common light sources, such as ultraviolet (UV) lamps, lasers, light-emitting diodes (LEDs), and halogen lamps are used for light-induced FP [8]; in particular, using infrared (IR) radiation as a light source in FP may offer some advantages [9]. IR radiation can facilitate the FP reaction as it utilizes both heat and light. This can lead to faster and more efficient polymerization than that achieved by the previous methods. In addition, IR radiation can penetrate deeper into materials than visible light can, allowing for a deeper and more uniform polymerization throughout the material.

Dicyclopentadiene (DCPD) is a monomer commonly used in FP because of its unique reactivity and ability to undergo frontal ring-opening metathesis polymerization (FROMP) [10]. Tributyl phosphite (TBP) is a commonly used radical initiator in FP because it can efficiently initiate the polymerization of DCPD and other monomers. In addition, a second-generation Grubbs catalyst (GC2) is commonly used in FP [4,6,7]. Upon using DCPD and TBP in FP, the resulting cross-linked polymer networks have been found to exhibit suitable mechanical properties, such as high tensile strength and elastic modulus [11], and excellent thermal stability, with a glass transition temperature of up to 219 °C, which could be useful for coating material [12]. Additionally, researchers demonstrated that the cross-linking density of poly (DCPD) networks could be controlled by varying the concentration of TBP, which allowed for the fine-tuning of the thermal and mechanical properties of the

†To whom correspondence should be addressed.
E-mail: korea1@kw.ac.kr

resulting polymers [2,13].

During the IR irradiation of FP, the photothermal effect is typically induced by a material known as an optical blackbody, which can absorb light across a broad range of wavelengths and convert it into heat [14]. Graphite, carbon black (CB), and metal nanoparticles, such as gold nanoparticles (AuNPs), are commonly used as optical blackbodies for this purpose [14,15]. CB has a higher surface area than graphite, which may make it more effective in absorbing and converting IR radiation into heat [16]. CB is also less expensive and more readily available than graphite, and it is widely used as a filler in the rubber industry [7]. However, there may also be some potential drawbacks in using CB as an optical blackbody for FP as it can lead to the formation of opaque or black polymers, which could present challenges for commercial applications that require transparency or other optical properties.

Therefore, in an FP reaction using CB as the photothermal agent, it may be challenging to achieve vivid or bright colors owing to the inherent color of CB and its potential for color interference. In this paper, we have proposed a new method for achieving variable color in the resulting polymer created through an FP reaction by combining CB and near-IR (NIR) light sources. Consequently, four-colored multilayers with a DCPD density variation across layers were created.

EXPERIMENTAL METHODS

1. Materials and CB/DCPD Preparation

DCPD (monomer), GC2 (catalyst), 5-ethylidene-2-norbornene (ENB, co-monomer), and phenylcyclohexane (PCH, solvent) were purchased from Sigma-Aldrich; TBP (initiator) was purchased from the Tokyo Chemical Industry; CB with a diameter of 30 nm was obtained from the Graphene Supermarket. All chemicals were used as received. DCPD is known to have a relatively high boiling point of around 170-180 °C, which indicates its ability to withstand elevated temperatures without significant evaporation or degradation. This property makes DCPD suitable for our resin system, where the resin temperature rises during initiation. Similarly, ENB also possesses a relatively high boiling point, typically around 165-175 °C. This co-monomer exhibits good thermal stability and can withstand the increased temperatures experienced during the initiation of the resin [4,6,7]. DCPD normally exists in a solid state because it has a melting point of ~33 °C. To lower this melting point below 25 °C, 5 wt% ENB (95 : 5 DCPD : ENB) was added [4,7]. CB/DCPD suspensions were prepared by ultrasonically dispersing DCPD with 0.0025, 0.005, and 0.01 wt% CB for 10 min. Catalyst solutions (GC2-x) were prepared by dissolving equimolar quantities of GC2 and TBP in 1 mL of PCH with various amounts of GC2 (20, 10, 5, and 2.5 mg of GC2 denoted by GC2-20, GC2-10, GC2-5, and GC2-2.5, respectively). Thereafter, 3 g of CB/DCPD was thoroughly mixed with the GC2-x solution in a glass test tube to homogenize the FP resin system.

2. Photothermal Performance of CB/DCPD Suspensions

The changes in the temperature profiles caused by NIR laser (808 nm, 3.5 W/cm^2, Joloy, LSR808NL) illumination were used to analyze the photothermal effect of CB/DCPD with various CB contents. To evaluate the features of heat propagation during the FP process and measure the maximum temperature reached via the photothermal effect, a thermal imaging camera (E5XT, FLIR) was used. To demonstrate its photothermal performance, 2 g of the CB/DCPD suspension was placed in a 4 mL quartz cuvette, and temperature profiles were recorded while the cuvette was exposed to NIR radiation for 10 min and then cooled for 10 min.

3. Preparation of Density Variation Multi-layers DCPD Resins

The temperature changes during the FP process were evaluated according to the amounts of CB and GC2-x under NIR irradiation. Twelve mixtures were prepared by mixing three different concentrations of CB with four different concentrations of GC2-x. A glass test tube was filled with 3 g of CB/DCPD/GC2-x and sub-

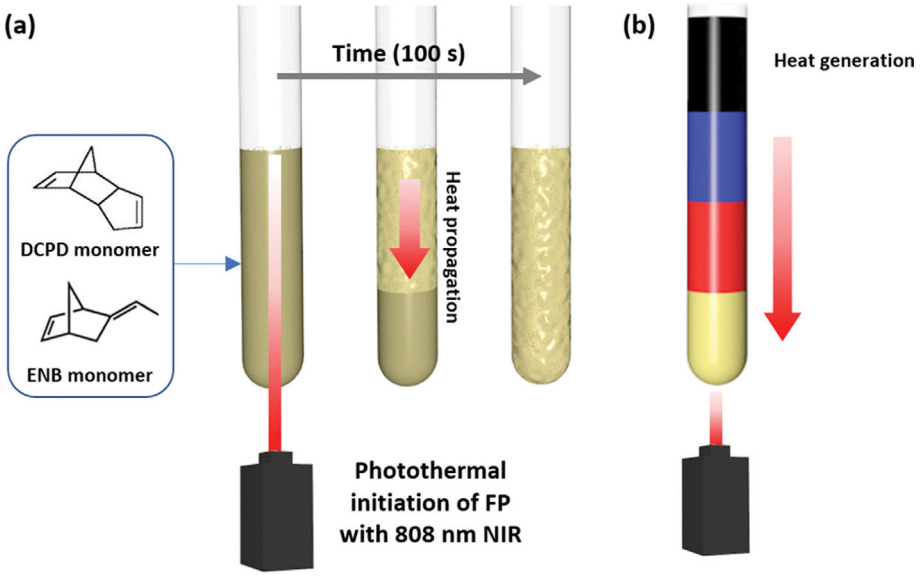

Fig. 1. Schematic of (a) photothermal initiation of FP of CB/DCPD and (b) density variation of DCPD with four layers under NIR laser irradiation.

jected to NIR irradiation up to the top of the tube (Fig. 1(a)). As a result of irradiating the NIR laser from both the side and below, it was observed that the irradiation from below led to a more uniform polymerization. This is attributed to the fact that when the laser is applied from below, it comes into closer contact with the solution, ensuring better distribution of the energy and promoting more homogeneous polymerization. The NIR laser was turned off as soon as the temperature increased significantly. Subsequently, the temperature decrease during the cooling time was measured until the solution returned to its initial temperature.

When CB was used as a photothermal agent in the FP process, the contrast of the black color of the DCPD resin could be adjusted by adjusting the CB content in the DCPD suspension; however, its color was not changeable. Thus, a density-variation DCPD solution was prepared to form the colored resins. Four solutions of different densities were prepared by adjusting the mixing ratio of DCPD and ENB. The glass test tube was filled with 0.8 g of four different densities of DCPD, which were 0.893, 0.936, 0.963, and 0.980 kg/m^3 from top to bottom of the test tube. CB was mixed only in the top-layer solution for initiating a photothermal effect. The heat generated by the CB under NIR irradiation was transferred to the bottom of the tube at the start of FP (Fig. 1(b)). The second and third layers were stained with methylene blue and acid red dye 1, respectively. If CB were placed in the bottom layer, the layers with a density variation solution would be mixed with the other layers in contact owing to natural convection. Therefore, CB was placed in the top layer.

RESULTS AND DISCUSSION

1. Photothermal Performance of CB/DCPD

The photothermal effect, which enables high-efficiency light-to-heat conversion, has piqued the interest of researchers in biology, chemistry, and medicine [17,18]. Metal nanoparticles and carbon materials (carbon nanotubes, graphite, and CB) with high light-absorption capacities are commonly used for photothermal effect research [19]. Owing to their excellent light absorption properties, AuNPs are commonly used as photothermal agents among these candidates. Localized surface plasmon resonance (LSPR), a distinguishing characteristic of AuNPs, is caused by the collective excitation of free electrons within AuNPs under light irradiation [20]. Its potential for enhancing chemical reactions has been demonstrated by LSPR-mediated photothermal heating under NIR irradiation, which is a nonradiative process [21]. Although AuNPs have shown great promise as photothermal agents, they are not economically comparable to CB.

CB is commonly used in the production of tires, inks, and plastics to improve their mechanical properties and provide color. Owing to its black color, CB exhibits broad UV-vis absorbance in the visible-to-NIR range [16]. Different mechanisms govern the generation of photothermal effects by CB and AuNPs upon exposure to NIR radiation. Amorphous carbon, in the form of CB, has high light scattering and absorption capabilities, allowing it to absorb NIR light. Through a nonradiative relaxation process, CB can transform the absorbed light energy into heat when exposed to NIR light [22]. Therefore, in this study, nanosized CB was used as a photothermal agent in the FP process because of its high cost-effectiveness, commercial availability, and uniform particle size (30-50 nm).

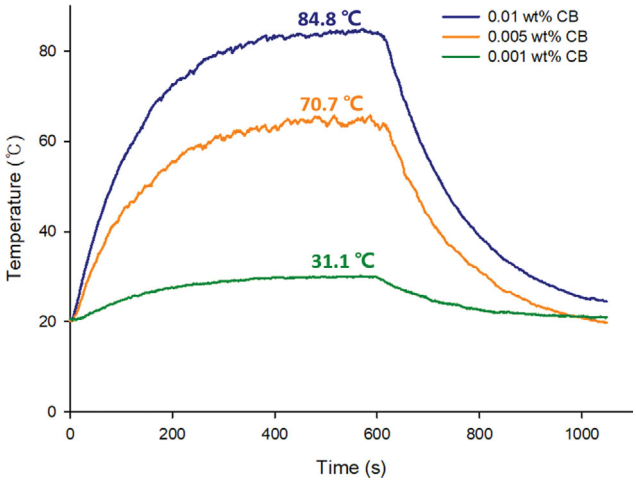

Fig. 2. Temperature profiles of CB/DCPD suspensions with different concentrations of CB under NIR irradiation.

The temperature profiles of the prepared CB/DCPD mixtures were assessed under NIR radiation. When heated, TBP breaks down into free radicals, which initiates a polymerization reaction in the monomer system. When NIR irradiation was applied to the CB/DCPD suspensions without TBP or GC2, resin curing did not occur; the resulting photothermal heating is shown in Fig. 2. As the proportion of CB in the DCPD suspensions increased, the maximum temperature increased up to ca. 85 °C. The required temperature for initiating FROMP of DCPD is ca. 60 °C [7]. The surface temperature of nanosized CB is likely higher than the bulk temperature of the suspensions, thus facilitating initiation at low temperature [23]. The temperature of the DCPD suspension with 0.001 wt% CB reached a maximum value of 31 °C, which was not sufficient for initiating FROMP of DCPD. Thus, a CB content of 0.0025 wt% or more is required for the FP reaction to occur. As a result, a relatively small amount of CB could be used to induce photothermal heating in this study. In the case of using a mercury vapor lamp (2-4 W/cm^2) as the light source [7], 1 wt% CB is required to increase the CB/DCPD suspensions' temperature to 60 °C or higher. The higher efficiency of the 808 nm NIR laser can be attributed to several factors, including the higher intensity of the NIR laser, the ability of CB to selectively absorb NIR light and efficiently convert it into thermal energy, and the resulting increase in surface temperature. While a mercury vapor lamp emits light across a broad spectrum, including wavelengths absorbed by CB, the intensity of the emitted light may not be as concentrated or focused as that of the 808 nm NIR laser. The higher intensity of the NIR laser enables more efficient energy transfer and subsequent heating of the CB/DCPD suspension. Therefore, the 808 nm NIR laser (3.5 W/cm^2) used in this study was considered to be an effective light source compared to a white lamp because NIR has the appropriate wavelength required to be absorbed by the blackbody (CB) and to be readily converted into thermal energy.

The photothermal conversion efficiencies of the CB/DCPD suspensions were evaluated. As shown in the temperature profiles,

when thermal equilibrium was reached after 10 min, the NIR laser was turned off, and the solution was cooled for 10 min. Based on the cooling curve shown in Fig. 2, the photothermal conversion efficiency (η) was determined as follows [17]:

$$\eta = \frac{hA(T_{max} - T_{surr}) - Q_{surr}}{I(1-10^{-A808})}, \quad (1)$$

where h is the heat-transfer coefficient, and A is the surface area. At thermal equilibrium, T_{max} and T_{surr} represent the maximum and surrounding temperatures, respectively. I represents the laser power, and A808 indicates the absorbance of the solutions at 808 nm [19-21]. Consequently, the photothermal efficiencies of the CB/DCPD suspensions containing 0.01, 0.005, and 0.001 wt% CB were calculated to be 85.4%, 64.4%, and 20.4%, respectively. Thus, the photothermal efficiency of the CB/DCPD suspension under NIR irradiation increased with the increase in the CB content.

2. Photothermal Initiation of FP for CB/DCPD/GC2-x

Photothermal initiation of FP in the CB/DCDP suspension was not observed even after NIR irradiation (Fig. 2). To initiate the FP reaction via NIR irradiation through photothermal effect, both GC2 catalyst and CB were required. GC2, specifically a ruthenium-based catalyst, plays a crucial role in FP processes. The role of GC2 is primarily associated with its ability to initiate the formation of radicals, which are key intermediates in the polymerization process [6,7]. In FP, the polymerization reaction propagates through a reactive front, which moves through the monomer system. GC2, as a catalyst, facilitates the initiation of this reaction by generating radicals from the initiator present in the system. These radicals then initiate the polymerization process by reacting with the monomer molecules, leading to the formation of polymer chains. Heat propagation during the FP reaction after the removal of the NIR light was observed in the IR images (Fig. 3). After photothermal initiation, the exothermic FP reaction propagated thermally, causing a sharp temperature increase to a maximum value of ~120 °C (Fig. 3). The excitation of GC2 and TBP caused by the NIR irradiation promoted the photoinitiation of FP [10], which occurred within 2 min. After FP initiation, the NIR laser was turned off, and the polymerization front continued to spread thermally in the absence of additional energy [7]. This method is appropriate for low-energy-consumption polymer curing because FP is driven by heat transfer rather than continuous irradiation. After the NIR laser was turned off, the maximum temperature was observed at the upper point in the IR image (Fig. 3). During the 80 s of thermal propagation, the point of maximum temperature moved downward toward the bottom of the tube. Light is typically irradiated downward from the lower side [7] or from the top to the bottom of the tube [11]. In this study, as shown in Fig. 3, light was irradiated vertically from bottom to top. In this configuration, the FP propagated from top to bottom and was successfully completed in a very short time. Note that even if CB was injected only into the top layer, the photothermal effect would cause the heat to propagate to the bottom of the tube, allowing FP to continue.

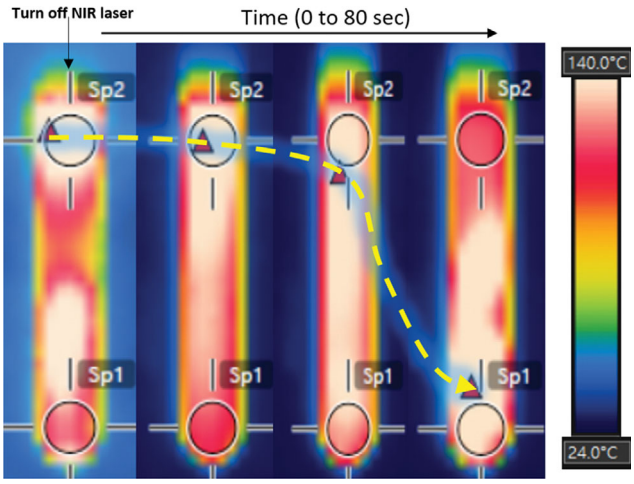

Fig. 3. IR images of CB/DCPD/GC2 resins after photothermal initiation of FP without further NIR irradiation (0 to 80 s). Red triangles represent the maximum temperatures.

The dependence of the maximum temperature and reaction start time on the amount of catalyst was investigated in a subsequent experiment. The glass test tube was filled with a single layer of the CB/DCPD/GC2-x suspension. When NIR was irradiated without photothermal particles, no significant temperature rise was observed. Therefore, NIR irradiation serves to initiate the photothermal effect specifically within the photothermal particles. As shown in Fig. 4(a), CB/DCPD/GC2-20 was found to exhibit a preheating curve for 80-100 s owing to the photothermal effect under NIR irradiation. This appears to be a temperature increase caused by the photothermal particles, as evidenced by the gradual temperature rise shown in Fig. 2. After preheating, the temperature increased rapidly as the exothermic FP reaction progressed because of the presence of the GC2 catalyst. The light was turned off after FP was observed to initiate thermal propagation without additional energy input. If the light is continuously provided, the propagated heat (reaction heat) and additional heat quickly produce vapors in the resins (light heat). Therefore, the light source should be turned off when the photothermal and exothermic reactions of the catalyst follow light irradiation.

In the case of the CB/DCPD/GC2-20 sample, the photoinitiation time decreased with increasing photothermal efficiency, which was due to the increasing CB content in the sample (Fig. 4(a)). For the CB/DCPD/GC2-x samples with a small amount of GC2 (Fig. 4(b)-4(d)), the photoinitiation time did not significantly depend on the amount of CB. However, the amount of catalyst affected the average preheating time during photothermal effect: 86.5, 117.9, 138.3, and 179.8 s for GC2-20 to GC2-2.5, respectively. The temperature at which the FP reaction began owing to spontaneous heat propagation was also determined by the amount of catalyst used: 50, 58, 60, and 62 °C for GC2-20 to GC2-2.5, respectively. Furthermore, the average rapid rise maximum temperature tended to drop as the catalyst concentration was reduced: 122.4, 119.1, 103.2, and 74.6 °C for GC2-20 to GC2-2.5, respectively. Therefore, the starting time and maximum temperature of the FP reaction strongly depended on the amount of catalyst used.

The temperature profiles of the CB/DCPD/GC2-x resins were similar. Therefore, based on Fig. 4, the rates of energy absorption (A, °C/s) and heat dissipation (B, s^{-1}) were calculated. The time-dependent temperature profiles for the laser-on and -off states can

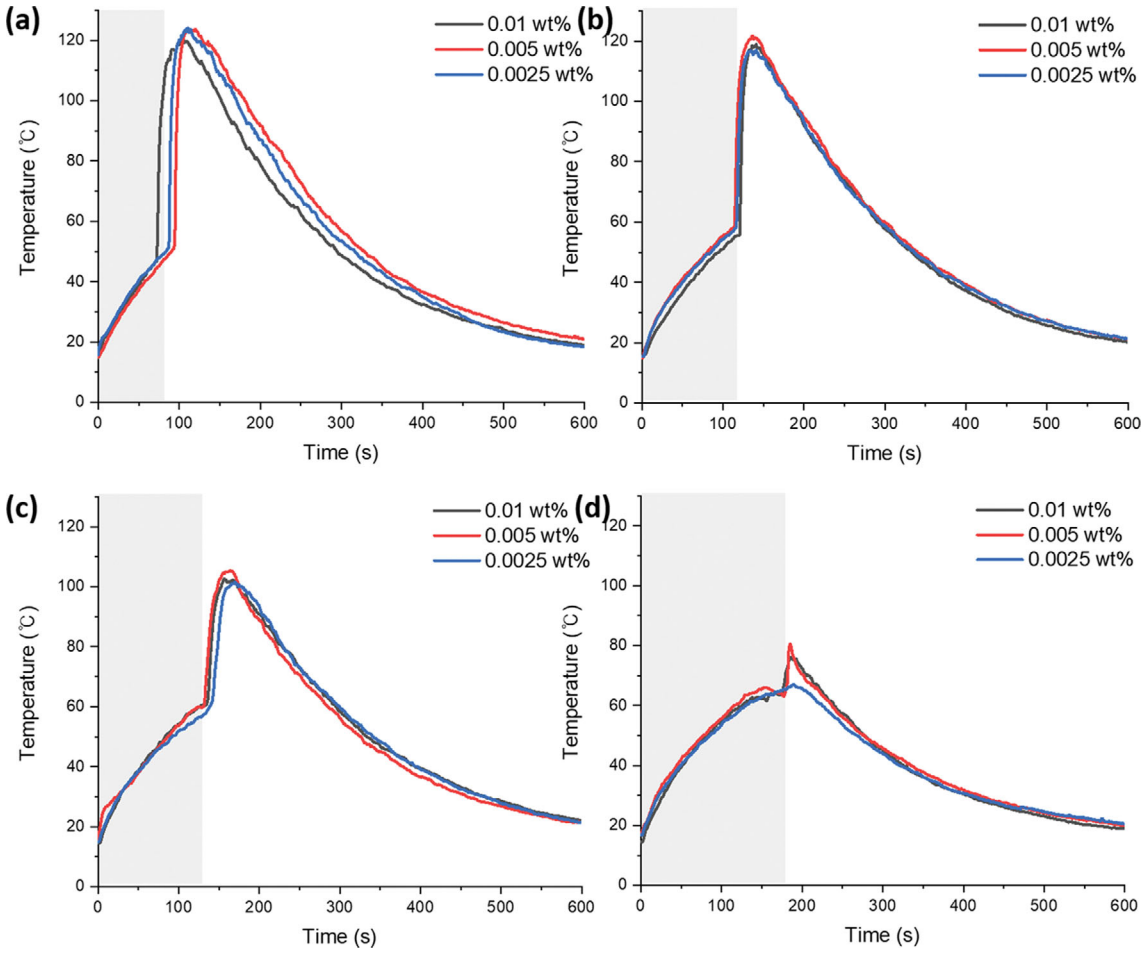

Fig. 4. Temperature profiles for FP of 0.0025-0.01 wt% CB/DCPD suspensions with different content of catalyst: (a) 20 mg (GC2-20), (b) 10 mg (GC2-10), (c) 5 mg (GC2-5), and (d) 2.5 mg (GC2-2.5). Gray section represents the time during which the samples were subjected to NIR irradiation.

Table 1. Rates of energy absorption (A, °C/s) and constant heat dissipation (B, s^{-1}) of CB/DCPD/GC2 resins with various concentrations of CB and GC2

CB contents	GC2-20		GC2-10		GC2-5		GC2-2.5	
	A	B	A	B	A	B	A	B
0.01 wt% CB	0.5336	0.0065	0.5029	0.0069	0.4945	0.0058	0.5124	0.0065
0.005 wt% CB	0.5080	0.0063	0.5004	0.0063	0.4549	0.0063	0.4982	0.007
0.0025 wt% CB	0.5238	0.0076	0.5222	0.0063	0.4481	0.0061	0.4402	0.0064

be defined using Eqs. (2) and (3) [24].

$$T(t) = T_0 + \frac{A}{B(1-e^{-Bt})}, \quad (2)$$

$$T(t) = T_0 + (T_{max} - T_0)e^{-Bt}, \quad (3)$$

where T_0 is the starting temperature, and T_{max} is the temperature after the laser is turned off. The values of A and B, which were determined from Fig. 4, are summarized in Table 1. These values slightly differed with the amount of GC2 and CB; for the CB/DCPD/GC2 resins, the values of A ranged from 0.50 to 0.53 °C/s and that of B was 0.006 s^{-1}. In comparison, in our previous work, hollow AuNPs dispersed in paint (HAuNPs@paint) yielded A of 0.292 °C/s and B of 0.0082 s^{-1} [17]. Thus, compared to HAuNPs@paint, CB/DCPD/GC2 exhibited higher energy absorption and heat dissipation rates under NIR irradiation. It is feasible then to rapidly increase and decrease the surface temperature of the CB/DCPD resins. The efficiency of light-to-heat conversion is related to the absorption efficiency of CB [22]. This result indicates that CB/DCPD can be used as a nanopigment and an efficient photothermal agent in paintings.

After completion of the FP reaction, the resulting samples were visually examined, as shown in Fig. 5. As the amount of CB in CB/DPCD/GC2-x decreased, the color of the final product changed from black to transparent. Vapors produced by a quick FP reaction

Fig. 5. CB/DCPD sticks obtained after FP with different contents of CB and catalyst.

remain in the resin if an excessive amount of catalyst is present. While the CB/DPCD/GC2-5 resin had no bubbles, the CB/DPCD/GC2-2.5 resin had a poor FP reaction and was soft enough to bend.

3. FP of Multi-layered Density Variation for Variable Colored Layers

The possibility of heat propagation from a top layer with CB to a bottom layer without CB was examined; 0.01 wt% CB was added only to the top layer, and all the layers were mixed with GC2-20 for the FP reaction, as shown in Fig. 1(b). NIR light was irradiated in a bottom-to-top direction, and the photothermal effect led to the generation of photoinitiated FP only in the top layer. In the previous experiments, light was removed when the FP reaction was initiated via the photothermal effect (Fig. 4). However, in this case of the density variation multilayered resin, as the bottom layer exhibited an absence of photothermal particles and insufficient heat propagation, curing did not occur in this layer. Therefore, the NIR irradiation was maintained until the FP reaction of the bottom layer began.

As shown in Fig. 6(a), the maximum temperatures of the layers from top to bottom were 155.4, 119.3, 110.8, and 100.3 °C, respectively. The FP reaction of the top layer started at t=18 s, and the second, third, and fourth layers reacted sequentially through heat propagation at t=23, 44, and 100 s, respectively. The NIR light was

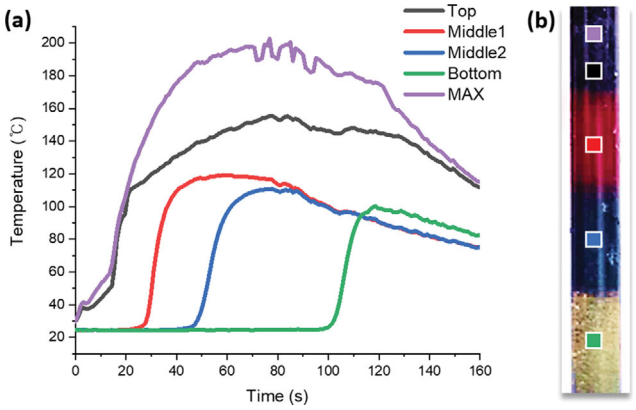

Fig. 6. Temperature profiles for FP of density variation four layered CB/DCPD suspensions under NIR laser irradiation with upward direction.

removed at the start of the FP reaction from the bottom layer. Finally, after the FP reaction, a four-colored poly (DCPD) resin was obtained, as shown in Fig. 6(b). Thus, the proposed method might be feasible for tuning the color of resins prepared using photoinitiated FP via photothermal effect. The maximum temperatures reached during laser exposure, as depicted in Fig. 6(a), exceeded the boiling points of DCPD and ENB after 30 s of exposure. This suggests that the monomers could potentially boil under these conditions. During the experimental process, it was found that a few bubbles formed exclusively in the top layer. However, these bubbles were successfully discharged to the upper layer, ensuring that the curing process proceeded without any issues. It is important to note that the presence of these bubbles did not compromise the overall effectiveness of the curing process.

CONCLUSIONS

This study investigated the use of CB as a cost-effective and efficient photothermal agent for photoinitiated FP processes under NIR irradiation. The temperature of the CB/DCPD suspensions increased with increasing CB content, and 0.0025 wt% or more of CB was required for FP initiation. The photothermal efficiencies of the CB/DCPD suspensions containing 0.01, 0.005, and 0.001 wt% CB were 85.4%, 64.4%, and 20.4%, respectively. As the amount of CB increased, the photothermal efficiency of the CB/DCPD suspensions under NIR irradiation increased. In the FP process of the CB/DCPD suspensions, FP was not initiated solely by the photothermal effect, but required both the GC2 catalyst and CB. Heat propagation during the FP reaction after the removal of the NIR light was observed using IR images. The maximum temperature and reaction start time were dependent on the amount of the catalyst used. The photoinitiation time decreased with increasing CB content, whereas the amount of catalyst affected the average preheating time and temperature at which the FP reaction began. Furthermore, the possibility of heat propagation from the top layer with CB to the bottom layer without CB was evaluated. Multilayered DCPD resins with different densities were prepared and NIR light was irradiated only on the top layer containing CB. The FP reac-

tion was initiated in the top layer, and heat propagated to the other layers, allowing them to cure. The maximum temperature of each layer was recorded, and the photoinitiated FP reaction occurred sequentially in each layer. These findings suggest that the proposed method can be used in the development of cost-effective and efficient photoinitiators for various applications, including the color tuning of resins.

ACKNOWLEDGEMENTS

This study was supported financially by the National Research Foundation of Korea (NRF-2022R1F1A1059495).

REFERENCES

1. Q. Li, H.-X. Shen, C. Liu, C.-F. Wang, L. Zhu and S. Chen, *Prog. Poly. Sci*., **127**, 101514 (2022).
2. J. Park and S.-Y. Kwak, *Commun. Chem*., **5**, 119 (2022).
3. I. D. Robertson, L. M. Dean, G. E. Rudebusch, N. R. Sottos, S. R. White and J. S. Moore, *ACS Macro Lett*., **6**, 609 (2017).
4. E. Goli, I. D. Robertson, P. H. Geubelle and J. S. Moore, *J. Phys. Chem. B*, **122**, 4583 (2018).
5. A. D. Tran, T. Koch, R. Liska and P. Knaack, *Monatsh. Chem*., **152**, 151 (2021).
6. P. J. Centellas, M. Yourdkhani, S. Vyas, B. Koohbor, P. H. Geubelle and N. R. Sottos, *Compos. Part A: Appl. Sci. Manuf.*, **158**, 106931 (2022).
7. L. M. Dean, A. Ravindra, A. X. Guo, M. Yourdkhani and N. R. Sottos, *ACS Appl. Polym. Mater*., **2**, 4690 (2020).
8. F. Petko, A. Świeży and J. Ortyl, *Polym. Chem*., **12**, 4593 (2021).
9. N. M. Tsegay, X.-Y. Du, K. Ma, Q. Li, C.-F. Wang and S. Chen, *J. Appl. Polym. Sci*., **135**, 45935 (2018).
10. I. D. Robertson, M. Yourdkhani, P. J. Centellas, J. E. Aw, D. G. Ivanoff, E. Goli, E. M. Lloyd, L. M. Dean, N. R. Sottos, P. H. Geubelle, J. S. Moore and S. R. White, *Nature*, **557**, 223 (2018).
11. D. G. Ivanoff, J. Sung, S. M. Butikofer, J. S. Moore and N. R. Sottos, *Macromolecules*, **53**, 8360 (2020).
12. Y. Gao, L. E. R. Koett, J. Hemmer, T. Gai, N. A. Parikh, N. R. Sottos and P. H. Geubelle, *ACS Appl. Polym. Mater*., **4**, 4919 (2022).
13. S. Zhao, J. Li, S. Ding, G. Zhu, S. Liu, W. Wu, P. Jin, M. An and Y. Luo, *Mater. Lett*., **321**, 132356 (2022).
14. B. A. Suslick, J. Hemmer, B. R. Groce, K. J. Stawiasz, P. H. Geubelle, G. Malucelli, A. Mariani, J. S. Moore, J. A. Pojman and N. R. Sottos, *Chem. Rev*., In Press (2023).
15. J. Hong, D. K. Hwang, C. Park and Y. Kim, *Korean J. Chem. Eng*., **36**, 1746 (2019).
16. S. K. Hazra, S. Ghosh and T. K. Nandi, *Appl. Therm. Eng*., **163**, 114402 (2019).
17. S. Jeong, J. Y. Park, J. M. Kim and Y. Kim, *Build. Environ*., **229**, 109970 (2023).
18. S. Han, Y.-J. Park, E.-J. Park and Y. Kim, *ACS Appl. Mater. Interfaces*, **11**, 8831 (2019).
19. W. Choi, J. Y. Park and Y. Kim, *J. Ind. Eng. Chem*., **95**, 120 (2021).
20. J. Kim, C. Park and Y. Kim, *J. Ind. Eng. Chem*., **107**, 376 (2022).
21. E. Park, R. Selvaraj and Y. Kim, *J. Ind. Eng. Chem*., **113**, 522 (2022).
22. X. Zuo, W. Yang, Z. Zhang, L. Song, H. Yan, C. Guan, J. Zhan, W. Zhu, H. Li, D. Zhang, X. Wen and Y. An, *Case Stud. Therm. Eng*., **38**, 102371 (2022).
23. O. Neumann, A. S. Urban, J. Day, S. Lal, P. Nordlander and N. J. Halas, *ACS Nano*, **7**, 42 (2013).
24. G. E. Craig, S. D. Brown, D. A. Lamprou, D. Graham and N. J. Wheate, *Inorg. Chem*., **51**, 3490 (2012).